Sustainable Energy & Fuels

ROYAL SOCIETY OF CHEMISTRY

PAPER

View Article Online
View Journal | View Issue

Open Access Article. Published on 07 Hlakubele 2023. Downloaded on 2025-11-06 21:12:56.
This article is licensed under a Creative Commons Attribution-NonCommercial 3.0 Unported Licence.

Check for updates

Cite this: *Sustainable Energy Fuels*, 2023, 7, 1930

Absolute environmental sustainability assessment of renewable dimethyl ether fuelled heavy-duty trucks†

Margarita A. Charalambous,[a] Victor Tulus,[a] Morten W. Ryberg,[b] Javier Pérez-Ramírez[a] and Gonzalo Guillén-Gosálbez *[a]

In recent years, liquid fuels from renewable carbon that can replace fossil ones with minimal infrastructure changes have attracted increasing interest in decarbonising the heavy-duty long-haul sector. Here we focus on dimethyl ether (DME), a promising alternative to diesel due to its high cetane number, oxygen content, and more efficient and cleaner propulsion that results in low particulate matter and sulphur oxide emissions. Going well beyond previous studies that quantified the environmental impact of DME, often in terms of global warming, here we evaluate DME use in heavy-duty trucks in the context of seven planetary boundaries, all essential for maintaining the Earth's stability. Focusing on several scenarios differing in the feedstock origin, we find that routes based on fossil carbon, either in the form of coal, natural gas, or captured CO_2 from fossil plants, would increase the greenhouse gas emissions relative to the business-as-usual. Only scenarios based on renewable carbon could reduce the impacts on climate change, while hydrogen from biomass gasification coupled with carbon capture and storage (CCS) and DME from biomass gasification with CCS could enable an environmentally sustainable operation within all the planetary boundaries. Overall, our work opens up new avenues for the environmental assessment of fuels considering the finite capacity of the Earth system to guide research and policy-making more sensibly.

Received 10th October 2022
Accepted 6th March 2023

DOI: 10.1039/d2se01409b

rsc.li/sustainable-energy

1 Introduction

Due to its large carbon emissions (*ca.* 24% of global greenhouse gas emissions in 2019), the transportation sector will be vital in meeting the climate goals.[1] This sector also emits nitrogen oxides (NO_x, N_2O) and PM, which are detrimental to human health and further call for more sustainable transportation modes.[2]

Battery electric and fuel cell vehicles hold good promise to decarbonise passenger vehicles,[3] yet their use in hard-to-abate transportation applications—trucks, ships, and planes—has been limited due to the lack of high-density batteries and sufficient charging infrastructure.[4–8] Consequently, in the short-term, heavy-duty (HD) trucks will still likely rely on the internal combustion engine (ICE).

Alternative sustainable fuels to diesel should exhibit a high cetane number and require minor modifications to the drive-train while maintaining or improving the engine efficiency and reducing exhaust emissions.[9] Recently, dimethyl ether (DME) has been gaining interest as it could provide a more efficient, soot-free, and sulphur-free combustion due to its oxygen content.[10–12] Notably, pure DME has good vaporisation and ignition performance, as well as a high cetane number (>55), making combustion in diesel engines faster, more complete, and silent while avoiding the exhaust gas treatment.[13,14] Additionally, it can be handled, transported, and stored as liquid petroleum gas and could be used in the same engine as diesel.[15]

During the past decade, DME has received increasing attention from truck manufacturers like Volvo, Mack, and Ford.[16,17] Companies such as Haldor-Topsoe, Mitsubishi Co., Lurgi (Air Liquide), JFE, MGC, and Total have been producing DME from natural gas for years, focusing more recently on greener DME,[18] while Oberon Fuels has created a modular DME technology from waste, excess electricity and CO_2.[19,20] Given the current level of investment, it is expected that by 2028 the market for DME fuel will reach 27 billion USD.[21]

Today, China holds the largest market share of DME production from coal, whereas a smaller share is obtained from natural gas, mainly in Europe and North America.[22] Alternatively, bio-DME is based on wood residues from forests,

[a]*Institute for Chemical and Bioengineering, Department of Chemistry and Applied Biosciences, ETH Zürich, Vladimir-Prelog-Weg 1, 8093 Zürich, Switzerland. E-mail: gonzalo.guillen.gosalbez@chem.ethz.ch*

[b]*Division for Quantitative Sustainability Assessment, Department of Management Engineering, Technical University of Denmark, Bygningstorvet, Building 116b, 2800 kgs. Lyngy, Denmark*

† Electronic supplementary information (ESI) available. See DOI: https://doi.org/10.1039/d2se01409b

This journal is © The Royal Society of Chemistry 2023

Open Access Article. Published on 07 Hlakubele 2023. Downloaded on 2025-11-06 21:12:56.
This article is licensed under a Creative Commons Attribution-NonCommercial 3.0 Unported Licence.

agricultural residues, and municipal solid waste.[19] At the same time, CO_2-based synthetic DME can be produced from CO_2 (captured from the air or at point sources) and hydrogen (from natural gas, biomass, or water electrolysis powered by renewables). Besides its role in transportation, DME could also become an energy carrier to store renewable energy.[23]

Assessing the economic and environmental performance of DME is essential to determine its sustainability level. Most DME studies based on process modelling,[24–29] and techno-economic assessments[30] focused on biomass,[29,31,32] and often studied the indirect route.[24–27] More recently, the direct conversion of CO_2-to-DME gained attention,[28,29,33,34] leading to the first pilot plants.[18]

Environmental studies of DME are scarce and mainly focus on global warming impacts.[12,19] Matzen and Demirel conducted a life-cycle assessment (LCA) of renewable methanol and DME from fermentation-based CO_2 and H_2 from wind-powered electrolysis, showing that they could reduce greenhouse gas emissions.[34] Lerner *et al.* investigated DME from natural gas, finding that its well-to-tank emissions could exceed those of diesel.[35] Silalertruksa *et al.* studied bio-DME from rice straw,[31] while Tomatis *et al.* analysed bio-DME from eucalyptus.[36] Fernández-Dacosta *et al.* also found that the end-of-life carbon emissions of DME from dry reforming of methane and CO_2-to-syngas could exceed those in diesel.[37] Furthermore, in the 2020 report of the Joint Research Institute of the European Commission, the well-to-wheels environmental assessment of DME originating from different sources (coal, natural gas, biomass, and electricity) was presented, focusing only on global warming impacts. The authors concluded that DME from coal and natural gas would increase the GHG emissions of the current diesel-fueled HD trucks. However, they pointed out the benefits that DME could provide when produced from residual feedstocks or *via* power-to-DME using renewable electricity.[12]

One key point in the studies above concerns the use of suitable environmental indicators. LCA has become the prevalent environmental assessment tool, yet its metrics are hard to interpret because they lack global thresholds to evaluate whether a technology is sustainable from a worldwide perspective. In recent years, absolute environmental sustainability assessments (AESA) have emerged that introduce limits to LCA indicators according to the planetary boundaries (PBs).[38] Notably, the PBs define limits on nine Earth-system processes (ESPs) that control the Earth's stability.[39,40] Based on this concept, Ryberg *et al.* developed a planetary boundary based life-cycle impact assessment (PB-LCIA) methodology to quantify impacts from the emissions and resources consumption of a system relative to the control variables of the PBs.[41,42]

Despite these efforts, PBs studies of industrial systems, in general, and fuels, in particular, are scarce. Ryberg *et al.* applied the PBs to the laundry washing industry[43] and a Danish utility company,[44] while Tulus *et al.* studied the PBs impact of chemicals.[45] Furthermore, following a similar approach, D'Angelo *et al.* evaluated low-carbon ammonia routes,[46] while Wheeler *et al.* investigated biomass supply chains.[47] Furthermore, Valente *et al.* assessed hydrogen fuel cell trucks relative to the PBs.[48]

For the first time, here we investigate whether DME from fossil and renewable carbon is sustainable in absolute terms using seven PBs. We find that, although renewable DME could reduce impacts substantially, most routes would still exceed at least one PB, which calls for optimised portfolios of renewable fuel technologies to decarbonise the HD road activities effectively.

2 Methodology

Our analysis focuses on low-carbon DME and its use in HD trucks as a pure fuel. Different energy sources and feedstocks were considered for CO_2, H_2, and biomass, leading to seven low-carbon scenarios that were benchmarked against the conventional DME from coal and natural gas, and the current diesel-fuelled HD trucking sector—business-as-usual (BAU)—(Fig. 1). We considered high technology readiness level alternatives (TRL > 7) available in an operational environment. The assessment was carried out using process simulation and LCA principles combined with the PBs concept, as described below.

2.1 Technologies and scenarios

We consider nine DME scenarios; two conventional scenarios based on coal and natural gas, five from CO_2 and H_2, and two based on biomass. The scenarios have been selected based on their relevance in the transportation sector. All the scenarios are assessed in terms of economic and environmental performance.

For all the DME scenarios, the production pathway follows the conventional two-step (or indirect) process, based on first producing methanol, followed by its dehydration to DME. DME can also be produced directly from syngas; however, only indirect DME commercial plants are under operation. Based on Bîldea *et al.*,[49] a process flowsheet of the DME production was developed in Aspen HYSYS v.11. The plant was scaled to produce 100 kt per year of DME with a final purity above 99.8% on a mass basis (flowsheet in Fig. S1 of the ESI).† The reaction takes place in the gas-phase on γ-alumina solid catalysts. The fixed-bed adiabatic reactor operates at 12 bar and 275–400 °C, obtaining 85% conversion. The outlet of the reactor is cooled down and enters the separation section. DME fuel is produced at 10 bar and 35 °C (99.9 wt%), consistent with its transportation and storage conditions.[50]

We assume that methanol can be obtained from coal, natural gas, CO_2 and H_2, or biomass. Conventional DME routes are based on coal gasification (coalDME scenario) and natural gas reforming (NGDME scenario) that dominate the market today. In the five CO_2 hydrogenation routes, CO_2 is captured from point sources at coal[51] or natural gas[52] plants or directly from air[53] (Coal, NG, and DAC, respectively). Furthermore, H_2 can be produced *via* electrolytic or thermochemical routes. Water electrolysis can be powered by onshore wind with wind turbines above 3 MW (Wind) and bioenergy combined with carbon capture and geological storage (BECCS). In the thermochemical route, H_2 is generated *via* biomass gasification with CCS (BTH). The flue gases are captured and geologically

Open Access Article. Published on 07 Hlakubele 2023. Downloaded on 2025-11-06 21:12:56.
This article is licensed under a Creative Commons Attribution-NonCommercial 3.0 Unported Licence.

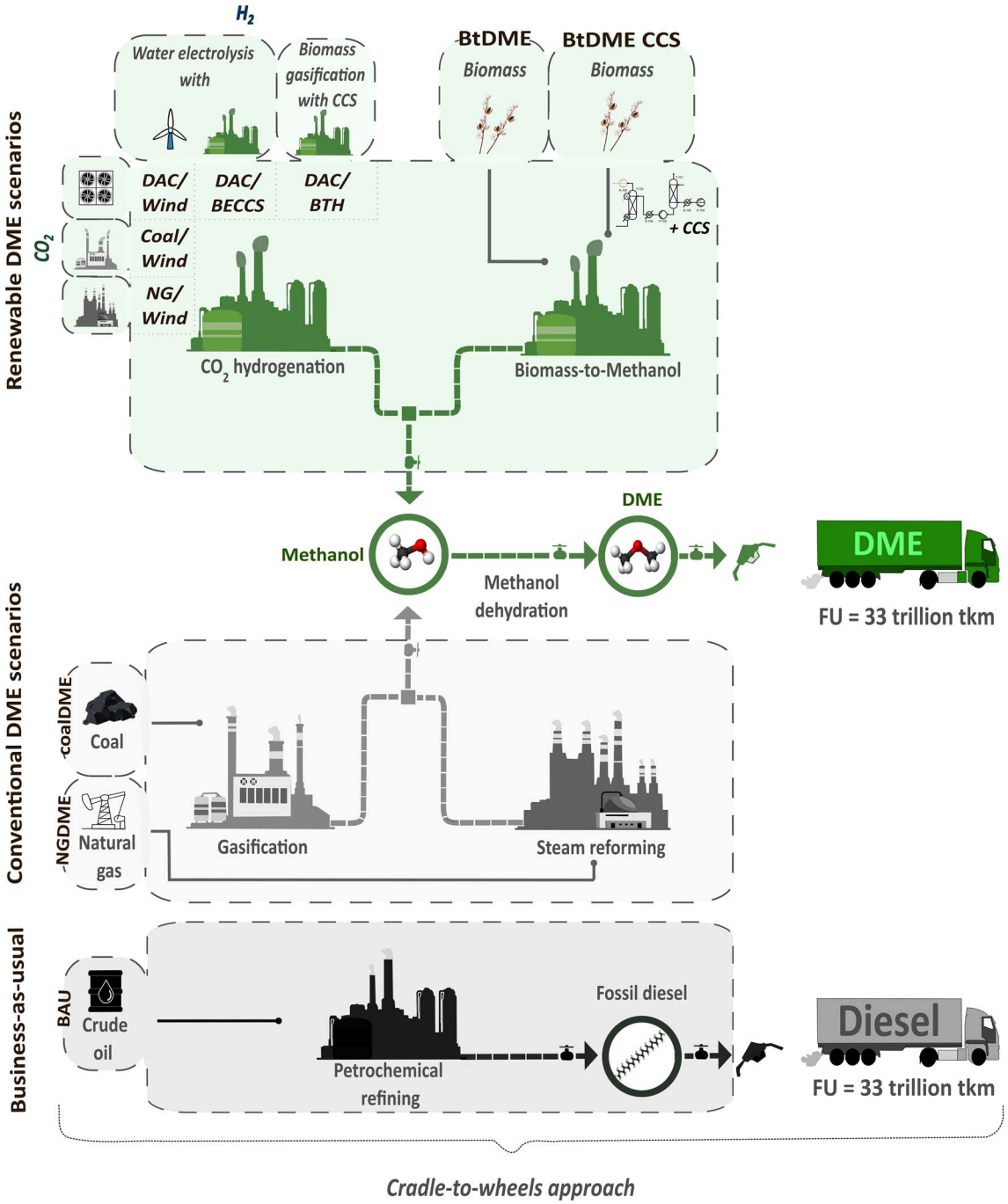

Fig. 1 Alternative scenarios analysed in this study. The functional unit is the global freight trucking demand supplied by the "business-as-usual" (BAU) scenario. DME is synthesised from coal, natural gas, CO_2 hydrogenation, or biomass. All the DME scenarios follow the indirect production route, where methanol is produced first, and then converted into DME. The scenarios are further described in Tables S1 and S2 of the ESI.†

stored.[54] The methanol synthesis process *via* CO_2 hydrogenation is described elsewhere.[55]

Finally, we consider the direct production of methanol from biomass-based syngas using cotton straw from agricultural activities as feedstock,[56] which is subsequently converted to DME through methanol dehydration (BtDME scenario). Biomass, acting as both a hydrogen and carbon source, is first pre-treated (drying and pelleting) and then converted to raw syngas through the gasification process, which takes place under high pressure and in the presence of air and high-pressure steam. Raw syngas is then conditioned and fed to the methanol reactor and purification unit. Furthermore, we captured all the carbon emissions by adding a CCS part to this process (BtDME CCS scenario). A furnace was included to burn all the purges, converting all the carbon emissions to CO_2, and a post-combustion capture process was simulated to capture

Open Access Article. Published on 07 Hlakubele 2023. Downloaded on 2025-11-06 21:12:56.
This article is licensed under a Creative Commons Attribution-NonCommercial 3.0 Unported Licence.

91% of the emissions. For all the alternative scenarios, the power grid covers the electricity demand of the processes, excluding the electricity for water electrolysis (which is produced from Wind and BECCS). This power grid corresponds to the electricity mix of 2019, and it is modelled based on the Stated Policies Scenario provided in the World Energy Outlook.[57]

2.2 Life-cycle assessment and planetary boundaries

We applied the general LCA methodology based on the four phases described in the ISO 14040/44 framework.[58,59]

2.2.1 Goal and scope definition phase. The analysis aims to assess the absolute environmental sustainability of fuelling the global HD truck activities with low-carbon DME based on different production pathways. The functional unit (FU) was defined as the global annual tonne kilometre (tkm) demand for HD activities estimated in 2020 by the International Energy Agency to be around 33 trillion tkm.[60] We adopted a cradle-to-wheel scope following an attributional approach. The system boundaries cover all upstream activities, *i.e.*, feedstock and energy inputs, production, and storage of DME at 10 bar (the delivery pressure for commercial DME trucks), including the fuel combustion in HD trucks.[50] The system boundaries also cover the manufacture of vehicles and roads.

2.2.2 Inventory analysis phase. The life-cycle inventory (LCI) calculations were implemented in SimaPro v9.2.0.2,[61] combining data from the background and foreground systems. All the inventories used in this work are presented in Tables S6–S23 of the ESI.†

2.2.2.1 Background system. Data from Ecoinvent v3.5 were used.[62] Regarding trucks, the BAU scenario considers the inventory named "transport, freight, lorry 16–32 metric ton, EURO6". Moreover, for the NGDME scenario, the "dimethyl ether production – RER" inventory was used.

2.2.2.2 Foreground system. Most of the mass and energy flows (*i.e.*, natural resources, raw materials from the technosphere, energy sources, by-products, and emissions) were retrieved from the literature, as described below, while others were generated using process simulation models. Notably, we developed a process simulation of the methanol dehydration step based on Bildea *et al.*,[49] which was implemented in Aspen HYSYS v.11, and a model for coal gasification to methanol, following Zachary Hoffman *et al.*[63] and González-Garay *et al.*,[64] implemented in Aspen PLUS v.11 (Fig. S2 of the ESI).† The carbon capture process for the direct conversion of biomass to methanol was simulated in Aspen HYSYS v.11 taking as feedstock the direct emissions from the BtDME scenario (Fig. S3 of the ESI).† The plant infrastructure was omitted. For the DME scenarios, the DME truck inventory was based on the BAU scenario, replacing the diesel fuel with DME and adjusting the associated tailpipe emissions. We calculated the DME consumption rate by assuming the same engine efficiency as in the BAU and considering the lower heating value of DME. We assumed complete combustion when estimating the CO_2 emissions, a 90% reduction of N_2O relative to the BAU, and 100% reduction of PM and SO_x emissions, as reported elsewhere.[65,66] Our foreground system also includes the emissions in the production of educts for methanol synthesis, *i.e.*, CO_2, H_2 and biomass, methanol from CO_2 hydrogenation and coal gasification, and DME.

2.2.2.3 Literature sources. Data for the production of H_2 (Wind, BECCS) were taken from Bareiß *et al.*,[67] based on water electrolysis in a 1 MW polymer electrolyte membrane (PEM) electrolyser. Data for gasket materials and membrane construction were retrieved from Koj *et al.*,[68] and Evangelisti *et al.*,[69] respectively. The inventory for the production of H_2 from biomass coupled with CCS (BTH) was retrieved from Susmozas *et al.*,[70] and Gasol *et al.*[71] For BECCS, data were retrieved from Oreggioni *et al.*[72] Capture of CO_2 from Coal follows Iribarren *et al.*,[51] which considers combustion capture with monoethanolamine (MEA) scrubbing of flue gases in a coal-fired power plant. In addition, data for CO_2 from NG, were retrieved from the simulation of Petrakopoulou *et al.*[73] Lastly, DAC, is based on Keith *et al.*,[74] which considers a commercial plant of Carbon Engineering capturing 1 Mt CO_2 per year. CO_2 from DAC is modelled as a negative output to portray the removal of atmospheric CO_2. In contrast, CO_2 from Coal and NG is modelled as a positive flow since it is removed from the flue gases and only reduces fossil emissions, thereby not contributing to a net removal of carbon from the air but rather preventing a fossil carbon flow. Methanol production *via* biomass gasification (BtDME scenario) follows Liu *et al.*,[75] and Bai *et al.*,[76] while CO_2 hydrogenation to methanol is based on Pérez-Fortes *et al.*[55] All the details on the inventories and process models, together with the main limitations and assumptions are included in Section 3 of the ESI.†

2.2.3 Impact assessment phase. In the life-cycle impact assessment (LCIA), we quantify the absolute environmental sustainability level of DME by converting the LCI elementary flows into impacts on the control variables (CVs) of the PBs. We apply the characterisation factors proposed by Ryberg *et al.* to quantify the impacts on six PBs;[42] climate change (CC), stratospheric ozone depletion (O_3D), ocean acidification (OA), biogeochemical flows (BGC), freshwater use (FWU), and land-system change (LSC). For the change in biosphere integrity (CBI), we followed Galán-Martín *et al.*[77] Atmospheric aerosol loading and novel entities were omitted due to the lack of suitable characterisation factors. The PBs and CVs used in this work and the safe operating space (SOS), *i.e.*, the ecological budget delimited by each PB, are presented in Table 1.

Considering a set of elementary flows e, for all scenarios s, and CVs of the PBs b, the environmental impact was calculated according to eqn (1):

$$\mathrm{EI}_{b,s} = \sum_{e \in E} \mathrm{LCI}_{e,s} \cdot \mathrm{CF}_{b,e} \;\; \forall \;\; b \in B, s \in S \tag{1}$$

$\mathrm{EI}_{b,s}$ represents the environmental impact of scenario s in each CV b. $\mathrm{LCI}_{e,s}$ is the elementary flow e (*i.e.*, feedstock requirements or emissions) in scenario s associated with the FU. All the values of $\mathrm{LCI}_{e,s}$ are calculated during phase two of the LCA. $\mathrm{CF}_{b,e}$, stands for the characterisation factor linked to CV b for elementary flow e.

Open Access Article. Published on 07 Hlakubele 2023. Downloaded on 2025-11-06 21:12:56.
This article is licensed under a Creative Commons Attribution-NonCommercial 3.0 Unported Licence.

Table 1 Planetary boundaries (PBs), control variable (CV) (*i.e.*, the biophysical variables used to quantify the status and limits of each specific PB), natural background level (NBL), and safe operating space (SOS)

Earth-system process	Control variable (CV)	Abbr.	PB[40] (NBL)[42]	SOS
Climate change	Atmospheric CO_2 concentration (ppm CO_2)	CC-CO_2	350 (278)	72
Climate change	Energy imbalance at the top of the atmosphere (W m^{-2})	CC-EI	1.0 (0)	1.0
Stratospheric ozone depletion	Stratospheric ozone concentration (DU)	O_3D	275 (290)	15
Ocean acidification	Carbonate ion concentration ($\Omega_{aragonite}$)	OA	2.7 (3.4)	69×10^{-2}
Biogeochemical flows	Global P cycle: flow from freshwater systems to the ocean (TgP per year)	BGC-P	11 (1.1)	9.9
Biogeochemical flows	Global N cycle: industrial and biological fixation of N (TgN per year)	BGC-N	62 (0)	62
Land-system change	Global area of forested land relative to original (%)	LSC	75 (10^2)	25
Freshwater use	Maximum consumptive blue water use, global (km^3 per year)	FWU	4.0×10^3 (0)	4.0×10^3
Change in biosphere integrity	Functional diversity (% BII loss)[80]	CBI	10 (0)	10

2.2.3.1 Uncertainty analysis. Uncertainties in the inventories are analysed by running the Monte Carlo sampling method implemented in SimaPro v9.2.0.2, considering 1000 scenarios and the default probability functions of the LCI flows defined in the software.

2.2.4 Interpretation phase. Finally, the results are interpreted in step four, and the main conclusions and recommendations are summarised. At this step, we analyse the impacts relative to the full-SOS. More precisely, we define the transgression level ($TL_{b,s}$) relative to the SOS in each scenario s and CV b as the ratio between the corresponding impact on the CV and the full-SOS as follows:

$$TL_{b,s} = \frac{EI_{b,s}}{SOS_b} \cdot 100\% \quad \forall\ b \in B,\ s \in S \tag{2}$$

We clarify that an impact above 100% indicates that the corresponding PB is surpassed in the scenario analysed. Notably, the SOS includes the maximum anthropogenic perturbation since it is the difference between the boundary and the natural background level. Assigning shares of the SOS requires applying downscaling principles, which are controversial.[78] Consequently, here, we avoid downscaling by referring to the impacts on the full-SOS (%). Therefore, we evaluate the sustainability of each scenario by focusing in the magnitude of the full-SOS that it takes up.

2.3 Economic assessment

The economic assessment considers only the OPEX, *i.e.*, the cost of raw materials and utilities, while neglecting the CAPEX due to its smaller contribution.[64] Only for the BtDME and BtDME CCS scenarios is the CAPEX considered since it represents 50–55% of the total production cost.[79] Also, the electrolyser cost is included in the levelised cost of hydrogen. Ultimately, the unitary cost of DME is computed as in eqn (1):

$$UC_{DME,s} = \sum_{u \in U} C^{UTI}_{u,s} \cdot \nu_{u,s} + \sum_{r \in R} C^{RAW}_{r,s} \cdot \mu_{r,s} \quad \forall s \in S \tag{3}$$

where $C^{UTI}_{u,s}$ represents the cost of utility u consumed in scenario s, and $C^{RAW}_{r,s}$ represents the cost of raw material r consumed in scenario s. Moreover, $\nu_{u,s}$ and $\mu_{r,s}$ are the amount of utility u and raw material r consumed in scenario s, respectively. The unitary cost of DME in each scenario ($UC_{DME,s}$) is expressed in USD per tkm. The costs of raw materials (CO_2, H_2, and biomass), heating utilities and electricity, were retrieved from the literature. The purchasing cost of the truck is omitted because we assume that it remains the same across scenarios. A sensitivity analysis was performed by varying the raw materials' and utilities' costs between best and worst values. The literature sources and cost ranges used for the economic analysis are provided in Table S24 of the ESI.†

3 Results

In this section, the environmental and economic assessment of the DME HD truck scenarios, explained in the previous sections, are presented and discussed relative to the diesel HD truck scenario (BAU).

3.1 Most DME routes exceed the safe operating space

Impacts on the PBs, as explained in eqn (1), are analysed and compared to the full-SOS (eqn (2)). The results are shown in Fig. 2. For a scenario to be environmentally sustainable, it should operate well beyond the SOS in all the PBs. In addition, for completeness, the "Global warming" in $CO_{2\text{-eq}}$, for all the scenarios, is included in the ESI (Fig. S6†).

Our results show that the current HD trucking sector (BAU scenario) is unsustainable. It alone transgresses the full-SOS in atmospheric CO_2 concentration (CC-CO_2) by a factor of 1.9 and energy imbalance at the top of the atmosphere (CC-EI) by a factor of 1.8 (operating in the high risk region) while taking 62% of the SOS in ocean acidification (OA) and 13% in change in biosphere integrity (CBI). The impact on the other PBs is negligible (<1%).

Similarly, all the DME scenarios but two exceed the full-SOS in at least one PB, often CC. DAC/BTH and BtDME CCS are the only absolute (environmentally) sustainable scenarios, showing impacts below the full-SOS in all the PBs. DAC/BTH, performs negative in the CC and OA PBs because of the carbon-negative H_2 used in DME production (recall that biomass gasification is coupled with CCS). However, due to the large amount of biomass needed for hydrogen production, DAC/BTH takes 43% of the CBI SOS. On the other hand, BtDME CCS is not carbon negative in CC and OA PBs because the amount of CO_2 captured

Open Access Article. Published on 07 Hlakubele 2023. Downloaded on 2025-11-06 21:12:56.
This article is licensed under a Creative Commons Attribution-NonCommercial 3.0 Unported Licence.

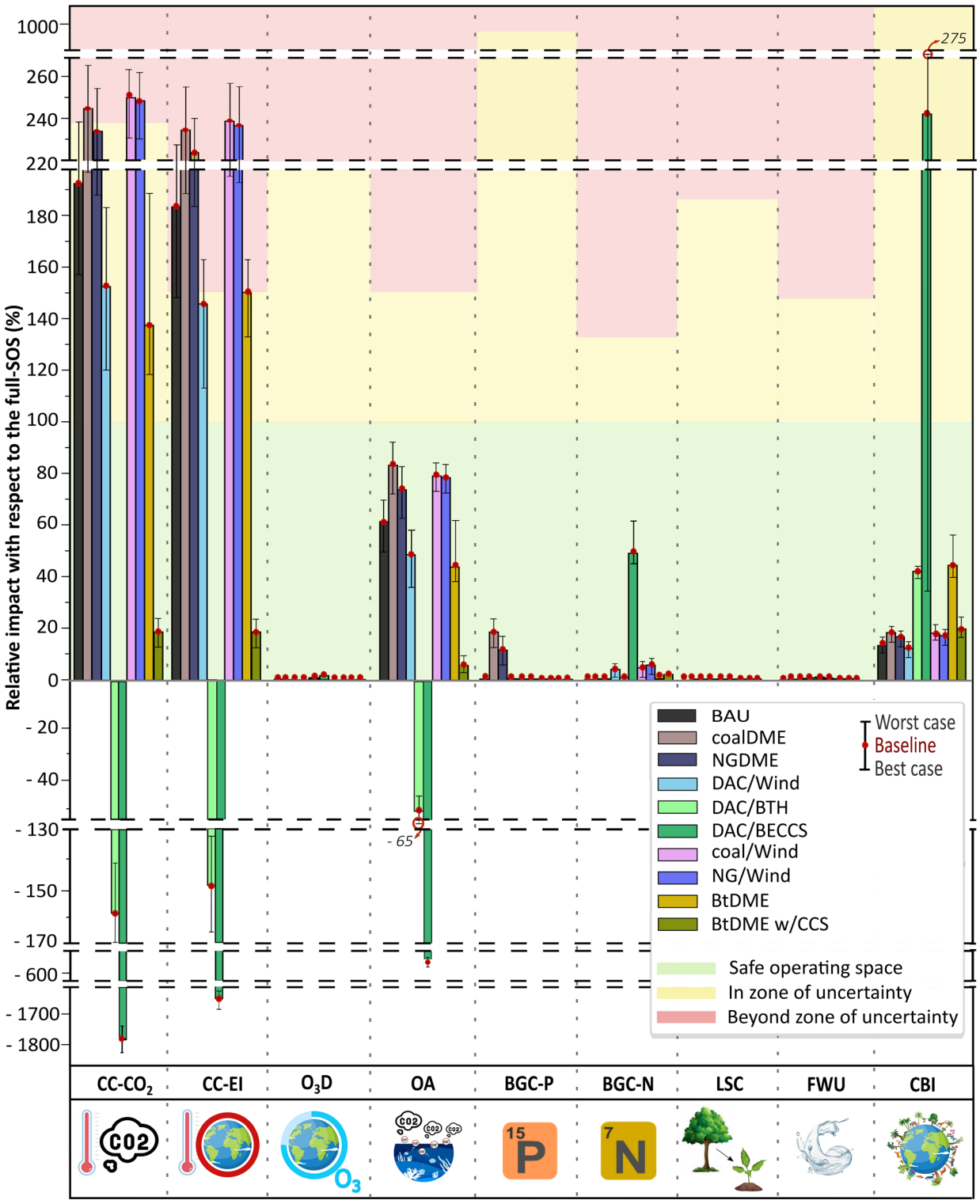

Fig. 2 Relative impact as the percentage of the full-SOS in all the scenarios (%). The shares of the SOS are shown for the current and proposed HD trucking sector, diesel-fuelled (BAU) and DME-fuelled HD trucks, respectively. Eight DME scenarios; two conventional (coalDME, NGDME), one biomass-based (BtDME), and five CO_2-based (DAC/Wind, DAC, BTH, DAC/BECCS, coal/Wind, NG/Wind). The abbreviations of the PBs are explained in Table 1.

cannot counterbalance the positive impacts of combustion emissions, heating requirements and truck infrastructure. However, it can decrease the current stresses of the BAU scenario in CC and OA.

Similarly, the DAC/BECCS scenario shows negative impacts on the GHG-related PBs due to the carbon-negative electricity used for water electrolysis. Nevertheless, DAC/BECCS performs very poorly in CBI (240%), because of the large land use

Open Access Article. Published on 07 Hlakubele 2023. Downloaded on 2025-11-06 21:12:56.
This article is licensed under a Creative Commons Attribution-NonCommercial 3.0 Unported Licence.

requirements needed for the woodchips biomass (originating from forest residues), and in the biogeochemical flows of nitrogen (BGC-N) (50%), due to the MEA during the carbon capture part.

The impact of the biomass-based scenarios on the land-system change (LSC) is very low because the CV considers forest transformation to cropland, while the BECCS assumed here is based on woodchips from forest residues which entails little forest transformation. Moreover, in the DAC/BTH scenario, the cultivation of poplar biomass does not contribute to LSC since it is implemented on a degraded land. The same low impacts occur in the freshwater use (FWU) PB, as there is no additional irrigation in BECCS and in the biogeochemical flows of P (BGC-P), where the boundary considers only the inflow of phosphorus from freshwater systems to the ocean. In this regard, we note that our results and, in particular, the occurrence of burden shifting strongly depend on the type of plantation, *e.g.*, dedicated willow or poplar plantations that need large amounts of fertilisers or irrigation would lead to larger impacts. Moreover, BTH, which relies on poplar biomass, has negligible impacts on the BGC-N and FWU PB.

None of the remaining scenarios operate within the full-SOS of climate change (coalDME, NGDME, coal/Wind, NG/Wind, DAC/Wind, BtDME), while most of them operate beyond the uncertainty zone in CC-EI PB. Notably, the conventional DME scenarios (coalDME and NGDME) are unsustainable, even performing worse than the BAU in all the PBs, *i.e.*, they transgress the CC-CO_2 PB by a factor of 2.5 and 2.4, respectively. Hence, replacing diesel with fossil DME is not environmentally appealing. Concerning the scenarios that use electrolytic H_2 powered by wind electricity, we find that, as expected, DAC/Wind outperforms coal/Wind and NG/Wind despite still lying within the uncertainty region for CC. Notably, DME scenarios originating from a fossil CO_2 source (coal/Wind and NG/Wind) would operate in the high-risk region. Hence, DME from green methanol powered by wind might be an interim solution to reduce the carbon emissions of transportation, but most likely not a long-term one.

Finally, the uncertainty analysis reveals that the largest uncertainty range corresponds to CBI. The DAC/BECCS scenario shows the largest variability. Specifically, in the best case, DAC/BECCS occupies only a small part of the SOS in the CBI PB (22%). The uncertainty stems from the large variations of biomass availability and CO_2 uptake in different regions of the world, depending on the type of land and growth conditions.

3.2 Combustion emissions and hydrogen dominate total impacts

Fig. 3 provides the breakdown of impacts in the most critical PBs, *i.e.*, those where the scenarios perform worst. The impacts are broken down into those embodied in "raw materials", and "utilities", and the ones linked to the "use phase". With regards to the "raw materials" category, we consider the impacts of the material feedstocks, *i.e.*, hydrogen, carbon dioxide, and biomass. "Utilities" refers to the impact embodied in the electricity and heat consumed. The "use phase" considers the

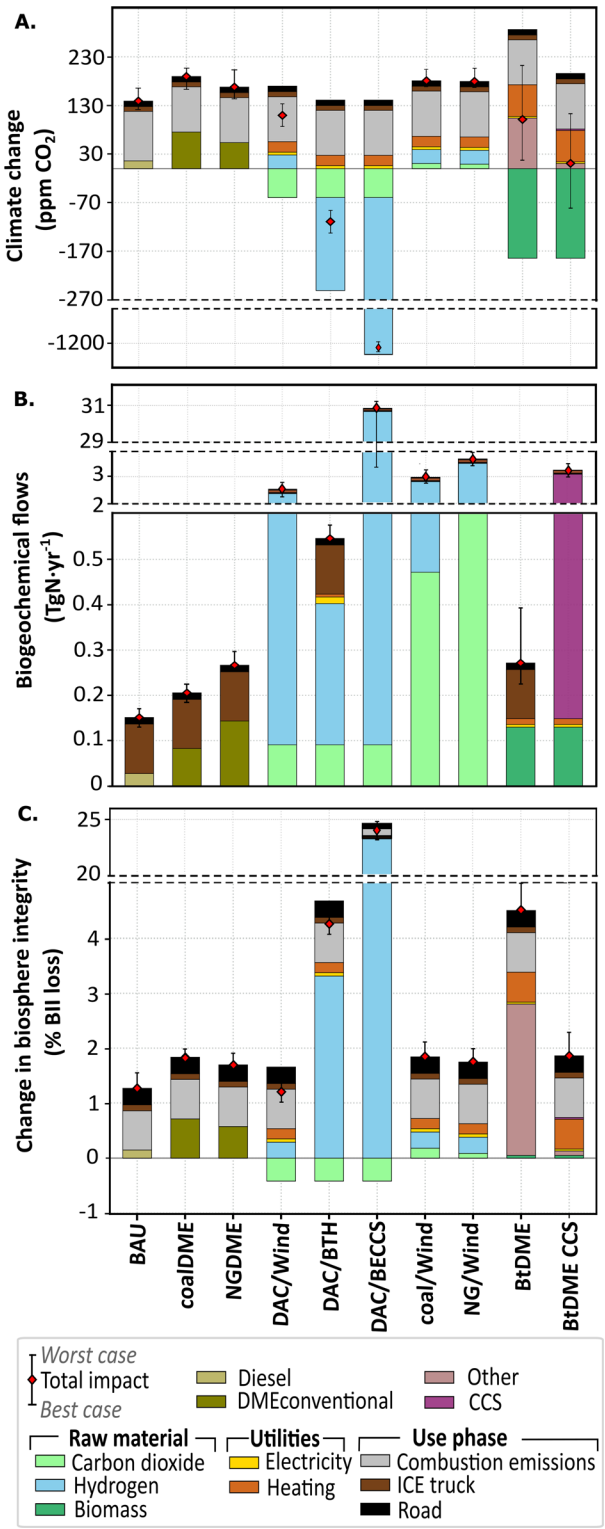

Fig. 3 Breakdown of impacts on the control variables of three ESPs per global annual tkm (33 trillion tkm); (A) climate change — CO_2 concentration, (B). Biogeochemical flows — N, and (C). Change in biosphere integrity. The total impact is indicated in red circles. Impact breakdown for the other PBs is included in the ESI (Fig. S3 and S4†), and the main contributions in Fig. S5.†

Open Access Article. Published on 07 Hlakubele 2023. Downloaded on 2025-11-06 21:12:56.
This article is licensed under a Creative Commons Attribution-NonCommercial 3.0 Unported Licence.

impact of the truck, the road, and the combustion emissions. "Other" includes the impacts from the production of ash, tar, wastewater, and direct emissions from the production of DME in the BtDME and BtDME CCS scenario, while "CCS" includes the impacts of the carbon capture and storage part of the BtDME CCS scenario. At the same time, "Diesel" represents the impact of the production of fossil diesel (cradle-to-tank emissions), and "DMEconventional" the impact of producing DME from coal and natural gas (cradle-to-tank emissions). Note that the infrastructure of roads and the ICE truck contributors are the same across scenarios.

In the CC-CO_2 PB (Fig. 3A), combustion emissions are the main driver (49–73% of the total impact depending on the scenario). They exceed the carbon emissions embodied in the fuel in all the scenarios (except for the BtDME scenario) and are larger in diesel than in DME (102 ppm CO_2 *vs.* 92 ppm CO_2, respectively) due to the lower carbon content of the latter (despite its lower energy content). Recall that in the DME scenarios, the impact embodied in the fuel includes the impact embodied in the methanol feedstock plus the impact of the dehydration process to produce DME. Furthermore, the carbon intensity of producing fossil diesel (*i.e.*, at cradle-to-gate) is smaller than that of DME from fossil resources (coalDME, NGDME, coal/Wind, NG/Wind). In contrast, it is bigger than that in the green DME alternatives, which are carbon negative (DAC/Wind — -2.3×10^{-12} ppm CO_2 kg_{DME}^{-1} —, DAC/BTH — -1.2×10^{-10} ppm CO_2 kg_{DME}^{-1} —, DAC/BECCS — -7.8×10^{-10} ppm CO_2 kg_{DME}^{-1} —, BtDME — -6.9×10^{-12} ppm CO_2 kg_{DME}^{-1} —, BtDME CCS — -5.7×10^{-11} ppm CO_2 kg_{DME}^{-1} —). The largest positive impact embodied in producing DME is found in the BtDME scenario, which requires significant heating (10 MJ kg^{-1} DME) and does not deploy CCS, resulting in substantial direct emissions (1.6 kg CO_2 kg_{DME}^{-1} and 0.16 kg CO_4 kg_{DME}^{-1} that are included in "Other"). The BtDME CCS scenario follows, with the heating requirements being the most prominent positive impacts. Conventional DME routes come next, with larger impacts in coalDME than in NGDME, due to the higher carbon monoxide (CO) and methane (CH_4) emissions of coal gasification to syngas. Their impact is similar to that in the scenarios relying on fossil CO_2 (coal/Wind, NG/Wind), followed by DAC/Wind, and finally, the DAC/BTH and DAC/BECCS scenarios, which are carbon-negative. CO_2 from DAC can almost offset the combustion emissions in the DAC scenarios, *i.e.*, the CO_2 captured is ultimately released back into the atmosphere during the combustion phase. However, recall that in the fossil CO_2 cases, there is no negative CO_2 flow during the fuel production phase to counterbalance the CO_2 release in the combustion phase, resulting in higher impacts.

Finally, H_2 from Wind is carbon positive and carbon negative when produced from biomass (BTH, BECCS). Notably, biomass scenarios (DAC/BTH and DAC/BECCS) remove CO_2 from the atmosphere; BTH could remove 191 ppm CO_2, whereas BECCS provides the most negative impacts, removing 1.3×10^3 ppm CO_2. The latter's potential is unrealistic as the current atmospheric CO_2 concentration is 415 ppm and the biomass growth would lead to the transgression of the CBI PB. However, by coupling the worst performing scenario in CC-CO_2 PB (coalDME) with DAC/BECCS, for example, it would still be possible to net remove CO_2 from the atmosphere. Most of the impacts from the Wind scenario—28 ppm CO_2 per global annual tkm—come from wind electricity (8.8×10^{-13} ppm kW h^{-1}), 90% of which results from the construction of wind turbines.

Regarding the BGC-N, in Fig. 3B, H_2 represents the main contribution (65–99%) for the CO_2-based scenarios (DAC/Wind, DAC/BTH, DAC/BECCS, coal/Wind, NG/Wind), while CCS for the BtDME CCS scenario. H_2 from BECCS performs worst due to the use of MEA during the carbon capture process. This is evident in Fig. S9 of the ESI,† where the impact breakdown of H_2 from BECCS is displayed. Around 99% of the impacts in BGC-N of electrolytic H_2 powered with BECCS come from MEA use (0.00673 kg MEA kW h^{-1} and 0.43 kg MEA/kg H_2). CCS in the BtDME CCS scenario follows, making the scenario perform 12-fold worse than the BtDME scenario due to the CCS addition and the MEA. H_2 from Wind comes next, where the main impacts originate from the manufacture of wind turbines (polyamide and copper hold 78% of the total impacts). This is higher than in BTH and BtDME, despite using nitrogen fertilisers for biomass growth. This is due to the high electricity demand for electrolytic water splitting. The breakdown of the electrolytic H_2 from Wind in BGC-N is included in Fig. S7 of the ESI.† Regarding the CO_2 sources, DAC performs 5.2 fold and 13 fold better than coal and NG, respectively, mainly due to the MEA use in the post-combustion capture processes (Fig. S9†).

Concerning CBI (Fig. 3C), the main contributors are combustion emissions and H_2 production, as well as "Other" in the BtDME scenario. The former is the top contributor in all the scenarios except for those based on biomass. Since this PB has two stressors, namely "GHG emissions" and "direct land use",[77,79,81] scenarios based on biomass (DAC/BTH, DAC/BECCS) result in high impacts because they are strongly connected to the land required during biomass growth. However, this is not the case for the BtDME scenario where the direct emissions during the methanol production from biomass (direct emissions are responsible for 98% of the impacts in "Other") are responsible for the biggest fraction of the impacts (65%). Here the "GHG emissions" stressor of CBI is the main contributor, while the "direct land use" of cotton straw is minimal. The impact of H_2 from BECCS is seven times that of BTH, making the former less appealing. Lastly, in the BtDME CCS scenario, the "Other" contribution is almost zero. This is because all the GHG emissions embodied in "Other" of the BtDME scenario are captured. More details on the breakdown between the two stressors contributing to CBI PB are provided in Fig. S10 and further explanations in Section 5.5 of the ESI.†

3.3 Hydrogen is the biggest contributor to the cost

The outcome of the economic analysis is shown in Fig. 4. The results are reported on a tkm basis, and on a "USD per MJ of fuel" basis in the ESI (Fig. S9†). On a tkm basis, coalDME would be the only scenario that can decrease the costs relative to the BAU scenario, while BtDME and BtDME CCS are economically appealing (5.2×10^{-2} USD per tkm and 5.5×10^{-2} USD per tkm, respectively). All the CO_2-based scenarios imply cost increases in the range of 1.8–3.9 fold.

Open Access Article. Published on 07 Hlakubele 2023. Downloaded on 2025-11-06 21:12:56.
This article is licensed under a Creative Commons Attribution-NonCommercial 3.0 Unported Licence.

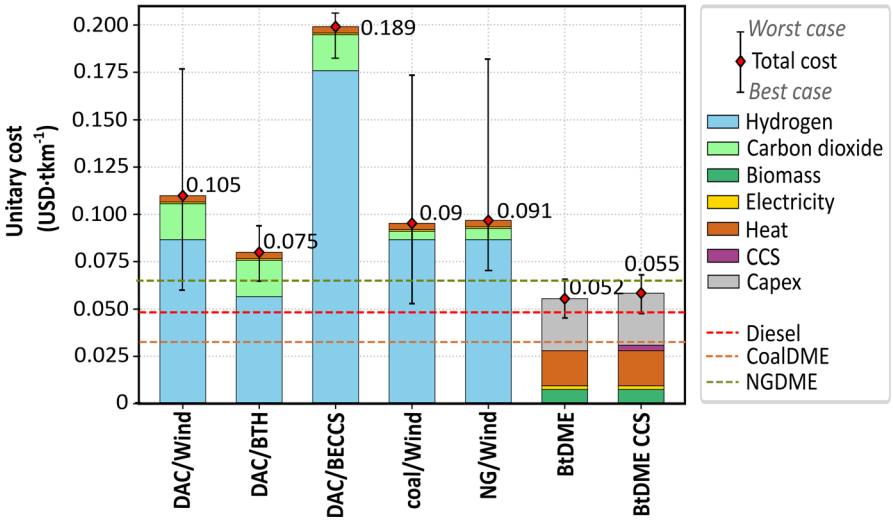

Fig. 4 Cost of DME per tkm calculated in Section 2.3. The error bars depict the best and worst scenario estimates according to the literature.

The biggest contributor to the costs is hydrogen, accounting for 71–91% of the total costs. Concerning the hydrogen sources, hydrogen from biomass (DAC/BTH) is the cheapest option, followed by Wind (DAC/Wind, coal/Wind, and NG/Wind), and lastly, BECCS (DAC/BECCS). Concerning CO_2 sources, DAC CO_2 is 4.3 and 3.2 times more expensive than CO_2 from Coal and CO_2 from NG, respectively. The high cost of DAC (1.8×10^{-2} USD per tkm) originates from its high energy demand compared to the capture in fossil plants, where the CO_2 concentration is much higher (15% and 8% *vs.* 0.04%, respectively) and, therefore, less energy is required.

Technology projections could strongly affect the economic viability of these scenarios. For example, improvements in the electrolyser and a decrease in the levelised cost of electricity could make DME more competitive.

When looking at the uncertainty range, it is evident that at the minimum cost extreme, coal/Wind, and DAC/Wind would be cheaper than fossil NGDME, while increasing the costs relative to fossil diesel only by 1.03–1.22 fold. Nevertheless, this economic competitiveness can only be realised in specific cases, *i.e.*, where abundant wind electricity is available to reduce capital investment costs. To break-even, the H_2 cost should be 1.7–2.6 USD $kg_{H_2}^{-1}$. Similarly, large-scale capture will decrease the costs of DAC and CO_2 from Coal and NG, pushing the total costs even lower. Hence synthetic DME could be economically competitive only if the costs of H_2 and CO_2 were reduced drastically.

3.4 Renewable carbon DME faces technical challenges

We next analyse the technical feasibility of the scenarios, focusing on biomass, CO_2, H_2, and power availability. The global deployment of the BtDME route would need 4.4×10^3 Mt per year of cotton straw, equivalent to 627–877 million ha.[56] For the CCU routes, 5.0×10^2 Mt per year of H_2 and 3.7×10^3 Mt per year of CO_2 would be required. The H_2 demand is 5.4 fold higher than today's annual production (93 Mt per H_2 (ref. 82)). Furthermore, 3.2×10^4 TW h of renewable electricity would be required to power just the electrolyser units, representing 15% of the global electricity production in 2019.[57]

Regarding CO_2, DAC could become a virtually unlimited source of CO_2. However, the technology is still in its infancy, capturing around 1.0×10^{-2} Mt CO_2 per year today and expected to reach 60 Mt CO_2 per year in 2030.[83] In addition, it will require 1.4×10^3 TW h of electricity and 19 EJ of heating, representing 55% and 15% of the annual electricity and heat production (from natural gas) in 2018, respectively. On the other hand, coal could provide around 1.0×10^5 Mt CO_2 per year, which can cover the CO_2 requirements for DME production, although only 13 Mt CO_2 per year are captured today.[84] However, using only Coal and NG CO_2 would not allow closing the carbon loop.[85]

As seen before, H_2 from BTH or electrolytic H_2 powered from BECCS have the potential to remove CO_2 from the atmosphere and, therefore, achieve carbon negative results. The requirements for poplar and woodchips from forest residues for these scenarios are 1.8×10^4 Mt per year and 3.4×10^4 Mt per year, respectively. The woodchips production will need 338 million hectares, representing one-third of the United States surface area, and 60 million hectares of poplar trees to satisfy BTH, equal to the surface of France and the Netherlands combined. Based on global estimations of 2050, the woodchips production based on the maximum global potential of BECCS is only 20% of the demand required.[86] Moreover, the degraded land availability for dedicated biomass production, *i.e.*, poplar biomass, amounts to 110 EJ per year, representing 38% of the land requirement needed in BTH.[86]

Lastly, the CCS routes (BECCS, BTH, BtDME CCS) require large amounts of CO_2 storage that might hinder their deployment. BECCS will need to store 54 Gt CO_2 per year, BTH 8.5 Gt CO_2 per year, and BtDME CCS 2.6 Gt CO_2 per year, adding up to the total CO_2 that CCS is supposed to deliver by 2050 to reach the 2 °C climate target (94 Gt CO_2 (ref. 87)).[88] The theoretical capacity for CO_2 storage in Europe, including saline aquifers,

Open Access Article. Published on 07 Hlakubele 2023. Downloaded on 2025-11-06 21:12:56.
This article is licensed under a Creative Commons Attribution-NonCommercial 3.0 Unported Licence.

hydrocarbon, and coal fields, is around 90 Gt.[89] This means that it would take less than two years for the underground storage of Europe to saturate with CO_2 from BECCS, around 10 years with CO_2 from the BTH one, and 35 years with CO_2 from BtDME CCS. Hence, a DME HD trucking sector fully relying on CCS would be unfeasible in the long term.

4 Conclusions

Here we quantified for the first time the absolute environmental sustainability of DME as an alternative fuel for the HD trucking sector using seven planetary boundaries (PBs). We found that only DME from renewable carbon has the potential to reduce the impact of diesel on the GHG-related PBs. In contrast, conventional DME from coal and natural gas or captured CO_2 from fossil plants would increase the GHG emissions relative to the diesel scenario, worsening the impact on climate change and ocean acidification. From the renewable carbon routes, only the one using hydrogen from biomass gasification with CCS would be absolute environmentally sustainable across all the PBs, despite exacerbating impacts mostly in biosphere integrity.

CoalDME, BtDME and BtDME CCS scenarios could be cost-competitive compared to fossil diesel, while the other routes are currently too expensive, when looking at the average cost values. Notably, the costs of DAC/Wind, DAC/BTH and coal/Wind could become more economically appealing at locations where the cost of Wind electricity and biomass is considerably lower. Moreover, the requirements for renewable power, land use, and carbon storage could hamper the technical feasibility of those DME routes relying on electrolytic H_2 from renewables, biomass, or CCS.

Overall, using only DME might not be a long-term option for the HD trucking sector. However, it could complement electric and hydrogen trucks in transitioning to a fully sustainable transport sector. Notably, until and beyond 2030, DME could be deployed in countries with abundant renewable energy and biomass, as part of technological portfolios optimised to collectively operate within PBs. On a methodological side, our work paves the way for future studies applying absolute sustainability criteria to the transport sector.

Acronyms

DME	Dimethyl ether
PBs	Planetary boundaries
CO_2	Carbon dioxide
GHG	Greenhouse gases
NO_x	Nitrogen oxides
N_2O	Dinitrogen monoxide
PM	Particulate matter
HD	Heavy-duty
ICE	Internal combustion engine
LCA	Life cycle assessment
AESA	Absolute environmental sustainability assessment
ESPs	Earth system processes
PB-LCIA	Planetary boundary life cycle impact assessment
ESI	Electronic supplementary information
BAU	Business-as-usual
FU	Functional unit
tkm	Tonne kilometer
LCI	Life cycle inventory
H_2	Hydrogen
MEA	Monoethanolamine
CVs	Control variables
SOS	Safe operating space
$CF_{b,e}$	Characterisation factor
$TL_{b,s}$	Transgression level
$EI_{b,s}$	Environmental impact
$UC_{DME,s}$	Unitary cost of DME
$C_{u,s}^{UTI}$	Utility cost in scenario s
$C_{r,s}^{RAW}$	Raw material cost in scenario s
$\nu_{u,s}$	Amount of utility u in scenario s
$\mu_{r,s}$	Amount of raw material in scenario s

Author contributions

Margarita A. Charalambous: formal analysis, investigation, methodology, software, writing – original draft, writing – review & editing, visualisation. Victor Tulus: software, conceptualisation, methodology, writing – review & editing. Morten W. Ryberg: conceptualisation, methodology, writing – review & editing. Javier Pérez-Ramírez: conceptualisation, methodology, writing – review & editing. Gonzalo Guillén-Gosálbez: conceptualisation, methodology, writing – review & editing.

Conflicts of interest

There are no conflicts to declare.

Acknowledgements

This publication was created as part of the NCCR Catalysis (grant 180544), a National Centre of Competence in Research funded by the Swiss National Science Foundation.

References

1 IEA, *Energy Technology Perspectives 2020*, 2020.
2 Z. D. Ristovski, B. Miljevic, N. C. Surawski, L. Morawska, K. M. Fong, F. Goh and I. A. Yang, *Respirology*, 2012, **17**, 201–212.
3 *World's First Fuel Cell Heavy-Duty Truck, Hyundai XCIENT Fuel Cell, Heads to Europe for Commercial Use – FuelCellsWorks*, https://fuelcellsworks.com/news/worlds-first-fuel-cell-heavy-duty-truck-hyundai-xcient-fuel-cell-heads-to-europe-for-commercial-use/, accessed 1 February 2021.
4 European Commission, *Sustainable and Smart Mobility Strategy*, 2020.
5 T. Walker, *Why the Future of Long-Haul Heavy Trucking Probably Includes a lot of Hydrogen*, 2021.
6 F. Chen, N. Taylor and N. Kringos, *Appl. Energy*, 2015, **150**, 109–119.

Open Access Article. Published on 07 Hlakubele 2023. Downloaded on 2025-11-06 21:12:56.
This article is licensed under a Creative Commons Attribution-NonCommercial 3.0 Unported Licence.

7 H. Liimatainen, O. van Vliet and D. Aplyn, *Appl. Energy*, 2019, **236**, 804–814.
8 I. Staffell, D. Scamman, A. Velazquez Abad, P. Balcombe, P. E. Dodds, P. Ekins, N. Shah and K. R. Ward, *Energy Environ. Sci.*, 2019, **12**, 463–491.
9 S. Schemme, R. C. Samsun, R. Peters and D. Stolten, *Fuel*, 2017, **205**, 198–221.
10 G. Thomas, B. Feng, A. Veeraragavan, M. J. Cleary and N. Drinnan, *Fuel Process. Technol.*, 2014, **119**, 286–304.
11 R. Song, K. Li, Y. Feng and S. Liu, *Energy Fuels*, 2009, **23**, 5460–5466.
12 M. Prussi, M. Yugo, L. De Prada and M. Padella, *JEC Well-To-Wheels report v5*, Publications Office of the European Union, Luxembourg, 2020.
13 S. Schemme, R. Can Samsun, R. Peters and D. Stolten, *Fuel*, 2017, **205**, 198–221.
14 G. A. Olah, A. Goeppert and G. K. S. Prakash, *Beyond Oil Gas Methanol Econ.*, 2nd edn, 2009, pp. 1–334.
15 C. Arcoumanis, C. Bae, R. Crookes and E. Kinoshita, *Fuel*, 2008, **87**, 1014–1030.
16 *Volvo Truck's plan to commercialize DME technology*, International Council on Clean Transportation, **https://theicct.org/blogs/staff/volvo-trucks-plan-commercialize-dme-technology**, accessed 6 April 2021.
17 *DME Fuel Truck Demonstration in New York City*, **https://oberonfuels.com/2017/01/12/oberon-fuels-mack-trucks-york-city-department-sanitation-customer-demonstration-dimethyl-ether-dme-powered-mack-truck/**, accessed 6 July 2021.
18 V. Dieterich, A. Buttler, A. Hanel, H. Spliethoff and S. Fendt, *Energy Environ. Sci.*, 2020, **13**, 3207–3252.
19 U. Lee, J. Han, M. Wang, J. Ward, E. Hicks, D. Goodwin, R. Boudreaux, P. Hanarp, H. Salsing, P. Desai, E. Varenne, P. Klintbom, W. Willems, S. L. Winkler, H. Maas, R. De Kleine, J. Hansen, T. Shim and E. Furusjö, *SAE Int. J. Fuels Lubr.*, 2016, **9**, 546–557.
20 *Oberon Fuels starts commercial production of rDME|Biomassmagazine.com*, **https://biomassmagazine.com/articles/18064/oberon-fuels-starts-commercial-production-of-rdme**, accessed 10 July 2021.
21 *Dimethyl Ether Market Size*, **https://www.verifiedmarketresearch.com/product/dimethyl-ether-market/**, accessed 10 July 2021.
22 *Dimethyl Ether Market by Raw Materials, Applications & by Geography – 2020|MarketsandMarkets*, **https://www.marketsandmarkets.com/Market-Reports/dimethyl-ether-market-1120.html**, accessed 4 February 2022.
23 P. Styring, G. R. M. Dowson and I. O. Tozer, *Front. Energy Res.*, 2021, **9**, DOI: **10.3389/FENRG.2021.663331/FULL**.
24 L. Zhang, J. Wang, P. Wu, Z. Hou, J. Fei and X. Zheng, *Chin. J. Catal.*, 2010, **31**, 987–992.
25 I. H. Kim, S. Kim, W. Cho and E. S. Yoon, in *Computer Aided Chemical Engineering*, Elsevier B.V., 2010, vol. 28, pp. 799–804.
26 L. Zhang, H. Zhang, W. Ying and D. Fang, *Can. J. Chem. Eng.*, 2013, **91**, 1538–1546.
27 Z. Bai, H. Ma, H. Zhang, W. Ying and D. Fang, *Pol. J. Chem. Technol.*, 2013, **15**, 122–127.
28 A. Hankin and N. Shah, *Sustainable Energy Fuels*, 2017, **1**, 1541–1556.
29 D. Liuzzi, C. Peinado, M. A. Peña, J. Van Kampen, J. Boon and S. Rojas, *Sustainable Energy Fuels*, 2020, **4**, 5674–5681.
30 S. Michailos, S. McCord, V. Sick, G. Stokes and P. Styring, *Energy Convers. Manage.*, 2019, **184**, 262–276.
31 T. Silalertruksa, S. H. Gheewala, M. Sagisaka and K. Yamaguchi, *Appl. Energy*, 2013, **112**, 560–567.
32 I. Landälv, R. Gebart, B. Marke, F. Granberg, E. Furusjö, P. Löwnertz, O. G. W. Öhrman, E. L. Sørensen and P. Salomonsson, *Environ. Prog. Sustainable Energy*, 2014, **33**, 744–750.
33 R. Vakili and R. Eslamloueyan, *Chem. Eng. Process.*, 2012, **62**, 78–88.
34 M. Matzen and Y. Demirel, *J. Cleaner Prod.*, 2016, **139**, 1068–1077.
35 A. Lerner, M. J. Brear, J. S. Lacey, R. L. Gordon and P. A. Webley, *Fuel*, 2018, **220**, 871–878.
36 M. Tomatis, A. Mahmud Parvez, M. T. Afzal, S. Mareta, T. Wu, J. He and T. He, *Fuel*, 2019, **254**, 115627.
37 C. Fernández-Dacosta, L. Shen, W. Schakel, A. Ramirez and G. J. Kramer, *Appl. Energy*, 2019, **236**, 590–606.
38 A. Bjorn, C. Chandrakumar, A. M. Boulay, G. Doka, K. Fang, N. Gondran, M. Z. Hauschild, A. Kerkhof, H. King, M. Margni, S. McLaren, C. Mueller, M. Owsianiak, G. Peters, S. Roos, S. Sala, G. Sandin, S. Sim, M. Vargas-Gonzalez and M. Ryberg, *Environ. Res. Lett.*, 2020, **15**, 8.
39 J. Rockström, W. Steffen, K. Noone, Å. Persson, F. S. Chapin, E. F. Lambin, T. M. Lenton, M. Scheffer, C. Folke, H. J. Schellnhuber, B. Nykvist, C. A. de Wit, T. Hughes, S. van der Leeuw, H. Rodhe, S. Sörlin, P. K. Snyder, R. Costanza, U. Svedin, M. Falkenmark, L. Karlberg, R. W. Corell, V. J. Fabry, J. Hansen, B. Walker, D. Liverman, K. Richardson, P. Crutzen and J. A. Foley, *Nature*, 2009, **461**, 472–475.
40 W. Steffen, K. Richardson, J. Rockstrom, S. E. Cornell, I. Fetzer, E. M. Bennett, R. Biggs, S. R. Carpenter, W. de Vries, C. A. de Wit, C. Folke, D. Gerten, J. Heinke, G. M. Mace, L. M. Persson, V. Ramanathan, B. Reyers and S. Sorlin, *Science*, 2015, **347**, 1259855.
41 W. Steffen, K. Richardson, J. Rockström, S. E. Cornell, I. Fetzer, E. M. Bennett, R. Biggs, S. R. Carpenter, W. De Vries, C. A. De Wit, C. Folke, D. Gerten, J. Heinke, G. M. Mace, L. M. Persson, V. Ramanathan, B. Reyers and S. Sörlin, *Science*, 2015, **347**, 6223.
42 M. W. Ryberg, M. Owsianiak, K. Richardson and M. Z. Hauschild, *Ecol. Indic.*, 2018, **88**, 250–262.
43 M. W. Ryberg, M. Owsianiak, J. Clavreul, C. Mueller, S. Sim, H. King and M. Z. Hauschild, *Sci. Total Environ.*, 2018, **634**, 1406–1416.
44 M. W. Ryberg, T. K. Bjerre, P. H. Nielsen and M. Hauschild, *J. Ind. Ecol.*, 2020, **25**(3), 765–777.
45 V. Tulus, J. Pérez-Ramírez and G. Guillén-Gosálbez, *Green Chem.*, 2021, **23**, 9881–9893.

 This journal is © The Royal Society of Chemistry 2023

Open Access Article. Published on 07 Hlakubele 2023. Downloaded on 2025-11-06 21:12:56.
This article is licensed under a Creative Commons Attribution-NonCommercial 3.0 Unported Licence.

46 S. C. D'Angelo, S. Cobo, V. Tulus, A. Nabera, A. J. Martín, J. Pérez-Ramírez and G. Guillén-Gosálbez, *ACS Sustainable Chem. Eng.*, 2021, **9**, 9740–9749.
47 J. Wheeler, Á. G. Martín, F. D. Mele and G. Guillén-Gosálbez, in *Computer Aided Chemical Engineering*, Elsevier B.V., 2020, vol. 48, pp. 1489–1494.
48 A. Valente, V. Tulus, Á. Galán-Martín, M. A. J. Huijbregts and G. Guillén-Gosálbez, *Sustainable Energy Fuels*, 2021, **5**, 4637–4649.
49 C. S. Bîldea, R. Győrgy, C. C. Brunchi and A. A. Kiss, *Comput. Chem. Eng.*, 2017, **105**, 142–151.
50 T. A. Semelsberger, R. L. Borup and H. L. Greene, *J. Power Sources*, 2006, **156**, 497–511.
51 D. Iribarren, F. Petrakopoulou and J. Dufour, *Energy*, 2013, **50**, 477–485.
52 F. Petrakopoulou, D. Iribarren and J. Dufour, *Greenhouse Gases: Sci. Technol.*, 2015, **5**, 268–276.
53 D. W. Keith, G. Holmes, D. St. Angelo and K. Heidel, *Joule*, 2018, **2**, 1573–1594.
54 A. Susmozas, D. Iribarren, P. Zapp, J. Linβen and J. Dufour, *Int. J. Hydrogen Energy*, 2016, **41**, 19484–19491.
55 M. Pérez-Fortes, J. C. Schöneberger, A. Boulamanti and E. Tzimas, *Appl. Energy*, 2016, **161**, 718–732.
56 N. Silanikove and D. Levanon, *Biomass*, 1986, **9**, 101–112.
57 IEA, *World Energy Outlook 2019*, 2019.
58 ISO, *Environmental Management: Life Cycle Assessment; Principles and Framework 14040*, ISO, 2006.
59 ISO, *Environmental Management: Life Cycle Assessment; Principles and Framework 14044*, 2006.
60 IEA, *The Future of Trucks*, 2017.
61 M. Goedkoop, M. Oele, J. Leijting, T. Ponsioen and E. Meijer, *Introd. to LCA with SimaPro*.
62 G. Wernet, C. Bauer, B. Steubing, J. Reinhard, E. Moreno-Ruiz and B. Weidema, *Int. J. Life Cycle Assess.*, 2016, **21**, 1218–1230.
63 Z. Hoffman, LSU Master's theses, Luisiana State University, 2005, pp. 1–97.
64 A. González-Garay, M. S. Frei, A. Al-Qahtani, C. Mondelli, G. Guillén-Gosálbez and J. Pérez-Ramírez, *Energy Environ. Sci.*, 2019, **12**, 3425–3436.
65 C. Arcoumanis, C. Bae, R. Crookes and E. Kinoshita, *Fuel*, 2008, **87**, 1014–1030.
66 G. Thomas, B. Feng, A. Veeraragavan, M. J. Cleary and N. Drinnan, *Fuel Process. Technol.*, 2014, **119**, 286–304.
67 K. Bareiß, C. de la Rua, M. Möckl and T. Hamacher, *Appl. Energy*, 2019, **237**, 862–872.
68 J. C. Koj, C. Wulf, A. Schreiber and P. Zapp, *Energies*, 2017, **10**, 860.
69 S. Evangelisti, C. Tagliaferri, D. J. L. Brett and P. Lettieri, *J. Cleaner Prod.*, 2017, **142**, 4339–4355.
70 A. Susmozas, D. Iribarren, P. Zapp, J. Linβen and J. Dufour, *Int. J. Hydrogen Energy*, 2016, **41**, 19484–19491.
71 C. M. Gasol, X. Gabarrell, A. Anton, M. Rigola, J. Carrasco, P. Ciria and J. Rieradevall, *Biomass Bioenergy*, 2009, **33**, 119–129.
72 G. D. Oreggioni, B. Singh, F. Cherubini, G. Guest, C. Lausselet, M. Luberti, H. Ahn and A. H. Strømman, *Int. J. Greenhouse Gas Control*, 2017, **57**, 162–172.
73 F. Petrakopoulou, D. Iribarren and J. Dufour, *Greenhouse Gases: Sci. Technol.*, 2015, **5**, 268–276.
74 D. W. Keith, G. Holmes, D. St. Angelo and K. Heidel, *Joule*, 2018, **2**, 1573–1594.
75 Y. Liu, G. Li, Z. Chen, Y. Shen, H. Zhang, S. Wang, J. Qi, Z. Zhu, Y. Wang and J. Gao, *Energy*, 2020, **204**, 117961.
76 Z. Bai, Q. Liu, L. Gong and J. Lei, *Appl. Energy*, 2019, **243**, 91–101.
77 Á. Galán-Martín, V. Tulus, I. Díaz, C. Pozo, J. Pérez-Ramírez and G. Guillén-Gosálbez, *One Earth*, 2021, **4**, 565–583.
78 M. W. Ryberg, M. M. Andersen, M. Owsianiak and M. Z. Hauschild, *J. Cleaner Prod.*, 2020, **276**, 123287.
79 S. Yang, B. Li, J. Zheng and R. K. Kankala, *J. Cleaner Prod.*, 2018, **205**, 364–374.
80 R. J. Scholes and R. Biggs, *Nature*, 2005, **434**, 45–49.
81 P. Jaureguiberry, N. Titeux, M. Wiemers, D. E. Bowler, L. Coscieme, A. S. Golden, C. A. Guerra, U. Jacob, Y. Takahashi, J. Settele, S. Díaz, Z. Molnár and A. Purvis, *Sci. Adv.*, 2022, **8**, 9982.
82 IEA, *The Future of Hydrogen*, 2019.
83 IEA, *Direct Air Capture*, 2021.
84 IEA, *Global Energy & CO_2 Status Report*, 2019.
85 *Learning from Petra Nova: What are the lessons for carbon capture?*, **https://www.nsenergybusiness.com/features/petra-nova-carbon-capture-project/**, accessed 9 August 2021.
86 IPCC, H. Chum, A. Faaij, J. Moreira, G. Berndes, P. Dhamija, H. Dong, B. Gabrielle, a G. Eng, O. M. Cerutti, T. Mcintyre, T. Minowa, K. Pingoud, K. Seyboth, P. Matschoss, S. Kadner, T. Zwickel, P. Eickemeier, G. Hansen and U. Kingdom, *Bioenergy*, 2012, 209–332.
87 IEA, *20 Years of Carbon Capture and Storage*, 2016.
88 S. Fuss, W. F. Lamb, M. W. Callaghan, J. Hilaire, F. Creutzig, T. Amann, T. Beringer, W. De Oliveira Garcia, J. Hartmann, T. Khanna, G. Luderer, G. F. Nemet, J. Rogelj, P. Smith, J. V. Vicente, J. Wilcox, M. Del Mar Zamora Dominguez and J. C. Minx, *Environ. Res. Lett.*, 2018, **13**, 063002.
89 T. Vangkilde-Pedersen, K. L. Anthonsen, N. Smith, K. Kirk, F. neele, B. van der Meer, Y. Le Gallo, D. Bossie-Codreanu, A. Wojcicki, Y. M. Le Nindre, C. Hendriks, F. Dalhoff and N. Peter Christensen, *Energy Procedia*, 2009, **1**, 2663–2670.